KSCE Journal of Civil Engineering

DOI 10.1007/s12205-019-0791-x

Tunnel Engineering

pISSN 1226-7988, eISSN 1976-3808
www.springer.com/12205

Analytical Prediction for Tunnel-Soil-Pile Interaction Mechanics based on Kerr Foundation Model

Zhiguo Zhang*, Chengping Zhang, Kangming Jiang***, Zhiwei Wang****, Yunjuan Jiang*****, Qihua Zhao******, and Minghao Lu*********

Received April 20, 2018/Revised December 29, 2018/Accepted January 31, 2019/Published Online March 12, 2019

Abstract

Existing analytical method to predict tunneling-induced pile deformation is generally based on the Winkler foundation model that neglects shear effects of soil, which is not sufficient for engineering practice. A simplified solution based on Kerr foundation model is presented in this study to investigate the tunnel-soil-pile interaction. In order to improve the accuracy of the prediction for tunneling-induced free-field movements, the cavity contraction theory is utilized in the first stage which receives a higher accuracy than the solution proposed by Loganathan and Poulos (1998). In the second stage, the soil free-field displacement is imposed on the existing pile, and the simplified solution for pile deformation governed by the disturbance of passive displacement is established based on the Kerr foundation model, which can take account of the soil shear effects. The applicability and accuracy of the simplified solution are then verified by several cases including the reported analytical solution, centrifuge modeling tests and observed data in situ. Good agreements are obtained in the comparative analyses, which demonstrates that the proposed solution can serve as an alternative approach for conservatively estimating tunneling-induced pile deformation in the preliminary design in clay. Furthermore, the parametric analysis associated with the pile deformation has also been performed. As a result, it is of primarily theoretical and practical significance to investigate the influence of soil shear effects on the tunnel-soil-pile interaction mechanics.

Keywords: *simplified solution, pile deformation, tunnel-soil-pile interaction, cavity contraction theory, Kerr foundation model*

1. Introduction

Owing to the fast urban development and the rapid growth of urban population, the operative infrastructures are exceedingly demanded in cities. Special attention is gathered on the growing awareness of further constructing the urban underground space. In current, tunnels are more and more frequently encountered in urban area in an attempt to relieve the burden of surface traffic. However, tunnel constructions inevitably cause soil stress changes and ground movements, which may adversely affect the existing structures. For example, tunnel excavation closely spaced to piles will unavoidably cause the piles to deform. To avoid possible damage to adjacent structures, two important aspects must be fully considered by the designer: the pile displacement induced by the deformation of surrounding soil in order to ensure structural serviceability; the additional forces imposed to the piles by the soil displacement in order to ensure structural integrity.

Current approaches for the free-field displacement and the tunnel-soil-structure interaction can be classified as the analytical derivation, the numerical simulation, and the in-situ test. Relevant researches include the estimation of the tunnel influences (Wang

*Associate Professor, School of Environment and Architecture, University of Shanghai for Science and Technology, Shanghai 200093, China; Visiting Professor, Key Laboratory of Urban Underground Engineering of Ministry of Education, Beijing Jiaotong University, Beijing 100044, China (Corresponding Author, E-mail: zgzhang@usst.edu.cn)
**Professor, Key Laboratory of Urban Underground Engineering of Ministry of Education, Beijing Jiaotong University, Beijing 100044, China (E-mail: chpzhang@bjtu.edu.cn)
***M.Sc. Student, School of Environment and Architecture, University of Shanghai for Science and Technology, Shanghai 200093, China (E-mail: 1309597582@qq.com)
****Assistant Professor, State Key Laboratory of Track Technology of High-Speed Railway, China Academy of Railway Sciences, Beijing 100081, China (E-mail: 240229397@qq.com)
*****M.Sc. Student, School of Environment and Architecture, University of Shanghai for Science and Technology, Shanghai 200093, China (E-mail: 957637374@qq.com)
******Professor, College of Environment and Civil Engineering, Chengdu University of Technology, Chengdu 610059, China (E-mail: zhqh@cdut.edu.cn)
*******M.Sc. Student, School of Environment and Architecture, University of Shanghai for Science and Technology, Shanghai 200093, China (E-mail: 982598492@qq.com)

et al., 2014; Liang *et al*., 2015, 2016, 2017; Lu *et al*., 2014, 2017), ground movements (Peck, 1969; Mair *et al*., 1993; Marshall *et al*., 2012; Miro *et al*., 2015; Zhang *et al*., 2017; Franza and Marshall, 2018), pile-group deformation (Jacobsz *et al*., 2004; Selemetas, 2005; Kaalberg *et al*., 2006; Marshall and Mair, 2011; Huang and Mu, 2012; Mu *et al*., 2012; Dias and Bezuijen, 2015; Franza *et al*., 2017; Shakeel and Ng, 2018), internal forces of piles (Kitiyodom *et al*., 2005; Huang *et al*., 2009; Ng *et al*., 2012; Basile *et al*., 2012; Soomro *et al*., 2015; Lueprasert *et al*., 2017), and pile failure (Matsuda *et al*., 2015).

Existing analytical solutions to evaluate tunnel-soil-pile interaction problem belong to two categories: 1) Complete 3D numerical simulation characterized by simulate the tunneling-disturbed soil together with the pile; and 2) simplified two-stage analytical method based on the assumption of the separation of the pile and the surrounding soil. Accordingly, the ground displacement can be solved in the first stage and the reported results are supplied on the pile structures. Three-dimensional finite element or finite difference analyses are widely employed in the first category to not only provide a complete three-dimensional analyses for the tunnel-soil-pile (or pipeline) interaction but also approximate the tunneling effects on the adjacent pile (Mroueh and Shahrour, 2002; Lee and Jacobsz, 2006; Cheng *et al*., 2007; Zhang and Zhang, 2013; Liyanapathirana and Nishanthan, 2016; Soomro *et al*., 2017; Chheng and Likitlersuang, 2018). Although the numerical analyses supported by commercial software are very helpful, the accuracy of the prediction heavily relies on modelling of practical conditions and soil behavior which are often ideally assumed. Moreover, numerical analyses consume repeating efforts for simulation and long running time, especially when complete parametric analyses need to be performed. To overcome the above-mentioned disadvantages, a simplified two-stage approach (Huang *et al*., 2009; Mu *et al*., 2012; Basile, 2012; Matsuda *et al*., 2015; Franza *et al*., 2017; Zhang *et al*., 2018) has been put forward to solve the excavation-soil-pile problem: In the first stage, estimating the tunneling-induced free-field displacement through an analytical solution; in the second stage, imposing the free-field displacement on the pile structure and assuming it as a beam to solve the pile deformation.

Regarding the two-stage method, a simplified foundation model is highly recommended for explicit understanding accepted by engineering designers. Winkler foundation model and Winkler-based models were commonly utilized by researchers in an attempt to solve problems associated with excavation. Nevertheless, the conventional Winkler model cannot take account of the continuity of soil and results in overestimation of bending moments and shear forces in the excavation. In addition, the Winkler-type model can only account for the elastic deformation but neglect the shear effect in the spring layer, which is crucial to soil with a large shear stiffness. Pasternak (1954) proposed a two-parameter foundation model concerning the defects of Winkler foundation model and it receives consistent favor among investigators (Zhang *et al*., 2018). A shear layer is added to the conventional model, which enables investigators to properly consider the continuity of soil and shearing effects of soil. However, in the Pasternak's foundation model, the shear layer is perfectly assumed to allow shear deformation and no compression deformation. Hence, Kerr foundation model was introduced with an extra spring layer so that the shear layer is located between two spring layers (Kerr, 1965, 1985; Kneifati, 1985; Avramidis and Morfidis, 2006). Owing to the extra spring layer, Kerr foundation model is designed for a more accurate approximation for the influence of lateral soil on the tunnel and is believed to better reflect the tunnel-soil-pile interaction. Furthermore, through adjusting the parameters, both Kerr model and Pasternak model achieve a closer evaluation to the field data. However, the solution based on the Kerr model is one step closer to the actual data.

In this study, a two-stage simplified solution is presented to estimate the pile deformation induced by tunneling. The soil-pile interaction mechanics is based on the Kerr three-parameter foundation model in which the shear effect of soil is well considered. In the first stage, the virtual image technique is adopted to solve the tunneling-induced free-field displacement, which is more accurate than that proposed by Loganathan and Poulos (1998) solution. In the second stage, the free-field displacement are applied to the pile structure, the simplified solutions for pile deformation governed by the disturbance of passive displacement are established based on the Winkler and Kerr foundation models, respectively. The simplified formula for the pile response induced by tunneling is obtained. The results are compared with that from reported approaches, measured data, and 3D numerical simulation. Furthermore, the influence of the concerned parameters of the Kerr foundation model on the pile deformation is also analyzed to further obtain the influencing rule for the tunnel-soil-pile interaction, including the pile diameter, the ground loss ratio and the tunnel-pile distance, as well as the soil spring coefficient and the thickness of soil shear layer.

2. Analytical Analyses

2.1 Free-Field Movements based on Cavity Contraction Theory

With respect to tunneling-induced soil displacement, current methods can be classified into three categories: empirical solution, analytical solution, and numerical solution. The numerical solution can predict the soil displacement accurately, but the concerned parameters are difficult to determine. In addition, the modelling effort (i.e., setting up mesh, materials, boundary conditions, imposing contraction, obtaining displacement at particular points, etc.) is reduced significantly when using analytical methods. The empirical method is simple, while the specific parameters remain to be determined according to the practical engineering, resulting in application limitations. The cavity contraction theory (Sagaseta, 1987; Verruijt and Booker, 1996) is

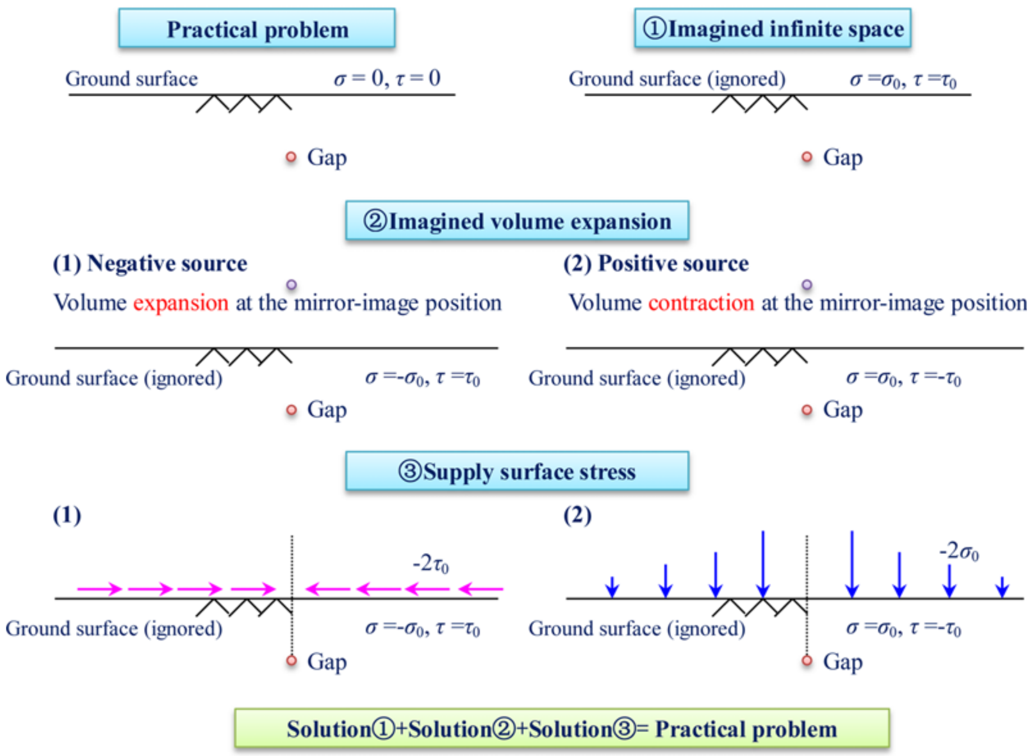

Fig. 1. Basic Steps for Cavity Contraction Theory

adopted in this paper. It is proved by existing researches that the cavity contraction theory can simulate the tunnel excavation process with higher precision (Yu and Rowe, 1999).

Tunnel excavation can be viewed as a model in the semi-infinite medium where centric shrinkage is generated in the cylindrical cavity under the in-situ stress. Based on the cavity contraction theory, the displacement distribution of the gap in infinite space is derived initially. Therefore, it is of intense necessity to transform the solution for infinite space into semi-infinite space problem, which can be completed based on the virtual image technique. The solving procedure is shown in Fig. 1: 1) The semi-infinite space problem is required to be converted into the a gap problem in infinite space where the ground surface is neglected and the soil is assumed as an infinite medium, and positive stress σ_0 and shear stress τ_0 are generated at the original position of the ground; 2) supposing that a new gap of the same size receives a volume expansion (or volume contraction) at the mirror position in the infinite space, the volume expansion can generate positive stress -σ_0 and shear stress τ_0 at the original position of the ground (or positive stress σ_0 and the shear stress -τ_0 for the volume contraction); and 3) the positive stress (or shear stress) of the first step and the second step in the original position of the ground can be counteracted, and the shear stress reaches $2\tau_0$ (or positive stress reaches $2\sigma_0$). To meet the actual boundary condition, the resulting additional shear stress (or positive stress) is applied to the ground surface at reversed value. The sum of the displacement followed by the above three steps is the solution of the actual problem.

2.1.1 Application of Cavity Contraction Theory in Plane Strain Problem

For shield tunneling, the three-dimensional problem can be simplified as a plane strain problem. According to the cavity contraction theory, the volume expansion at the mirroring point is resolved in the solution. The displacement component $U_{x1}(x)$, $U_{y1}(y)$, and $U_{z1}(z)$ generated at the point $(x, 0, z)$ from the gap with a contraction radius a of the point $(x_0, 0, z_0)$ in infinite space can be expressed as:

$$\left.\begin{aligned} U_{x1}(x) &= -\frac{a^2}{2}\frac{x-x_0}{r_1^2} \\ U_{y1}(y) &= 0 \\ U_{z1}(z) &= -\frac{a^2}{2}\frac{z-z_0}{r_1^2} \end{aligned}\right\} \tag{1}$$

where $r_1 = [(x-x_0)^2 + (z-z_0)^2]^{1/2}$.

The displacement component $U_{x2}(x)$, $U_{y2}(y)$, and $U_{z2}(z)$ generated at the point $(x, 0, z)$ from the volumetric expansion with a contraction radius a of the point $(x_0, 0, z_0)$ in infinite space can be expressed as:

$$\left.\begin{aligned} U_{x2}(x) &= \frac{a^2}{2}\frac{x-x_0}{r_2^2} \\ U_{y2}(y) &= 0 \\ U_{z2}(z) &= \frac{a^2}{2}\frac{z+z_0}{r_2^2} \end{aligned}\right\} \tag{2}$$

where $r_2 = [(x-x_0)^2 + (z+z_0)^2]^{1/2}$.

The displacement components of the *x*-axis, *y*-axis and z-axis, $U'_x(x)$, $U'_y(y)$ and $U'_z(z)$ are obtained through Eqs. (1) and (2):

$$\left.\begin{aligned} U'_x(x) &= -\frac{a^2}{2}\left(\frac{x-x_0}{r_1^2} - \frac{x-x_0}{r_2^2}\right) \\ U'_y(y) &= 0 \\ U'_z(z) &= -\frac{a^2}{2}\left(\frac{z-z_0}{r_1^2} - \frac{z+z_0}{r_2^2}\right) \end{aligned}\right\} \tag{3}$$

The additional shear strain $\gamma(x)$ generated at the ground surface can be obtained:

$$\gamma(x) = \left(\frac{\partial S'_x}{\partial z} + \frac{\partial S'_z}{\partial x}\right)_{z=0} = -4a^2 \frac{z_0(x-x_0)}{\left((x-x_0)^2 + z_0^2\right)^2} \tag{4}$$

In addition, the corresponding additional shear stress $\tau(x)$ is obtained as:

$$\tau(x) = G\gamma = -4Ga^2 \frac{z_0(x-x_0)}{\left((x-x_0)^2 + z_0^2\right)^2} \tag{5}$$

Reversing the shear stress at the ground surface and imposing it on the surface, the displacement components $U_{x3}(x, z)$, $U_{y3}(x, z)$, and $U_{z3}(x, z)$ can be obtained through the integration of the Cerruti solution:

$$\left.\begin{aligned} U_{x3}(x,z) &= -a^2 \frac{(x-x_0)}{r_2^2}\left[1 - 2\frac{z(z+z_0)}{r_2^2}\right] \\ U_{y3}(x,z) &= 0 \\ U_{z3}(x,z) &= a^2 \frac{z}{r_2^2}\left[1 - 2\frac{(x-x_0)^2}{r_2^2}\right] \end{aligned}\right\} \tag{6}$$

Substituting Eqs. (1) and (2) into Eq. (6), the final solution for $U_x(x, z)$, $U_y(x, z)$, and $U_z(x, z)$ generated at an arbitrary point $(x, 0, z)$ from the gap with a contraction radius a of the point $(x_0, 0, z_0)$ in semi-infinite ground (plane-strain) can be expressed as:

$$\left.\begin{aligned} U_x(x,z) &= U_{x1} + U_{x2} + U_{x3} \\ &= -\frac{a^2(x-x_0)}{2}\left(\frac{1}{r_1^2} + \frac{1}{r_2^2}\right) + \frac{2a^2 z(x-x_0)(z+z_0)}{r_2^4} \\ U_y(x,z) &= U_{y1} + U_{y2} + U_{y3} = 0 \\ U_z(x,z) &= U_{z1} + U_{z2} + U_{z3} \\ &= -\frac{a^2}{2}\left(\frac{z-z_0}{r_1^2} - \frac{3z+z_0}{r_2^2}\right) - \frac{2a^2 z(x-x_0)^2}{r_2^4} \end{aligned}\right\} \tag{7}$$

To obtain the displacement solution generated by unit volume gap, the displacement components of Eq. (7) is demanded to be divided by volume πa^2. Consequently, the final solution for the displacement component $u_x(x, z)$, $u_y(x, z)$, and $u_z(x, z)$ generated at the point $(x, 0, z)$ from the gap per unit volume of the point $(x_0, 0, z_0)$ in semi-infinite ground (plane-strain) can be obtained:

$$\left.\begin{aligned} u_x(x,z) &= -\frac{(x-x_0)}{2\pi}\left(\frac{1}{r_1^2} + \frac{1}{r_2^2}\right) + \frac{2z(x-x_0)(z+z_0)}{\pi r_2^4} \\ u_y(x,z) &= 0 \\ u_z(x,z) &= -\frac{1}{2\pi}\left(\frac{z-z_0}{r_1^2} - \frac{3z+z_0}{r_2^2}\right) - \frac{2z(x-x_0)^2}{\pi r_2^4} \end{aligned}\right\} \tag{8}$$

For the ground surface (z = 0), the displacement components $u_{x0}(x, 0)$, $u_{y0}(x, 0)$, and $u_{z0}(x, 0)$ generated from the gap per unit volume are:

$$\left.\begin{aligned} u_{x0}(x,0) &= \frac{-(x-x_0)}{\pi[(x-x_0)^2 + z_0^2]} \\ u_{y0}(x,0) &= 0 \\ u_{z0}(x,0) &= \frac{z_0}{\pi[(x-x_0)^2 + z_0^2]} \end{aligned}\right\} \tag{9}$$

2.1.2 Application of Cavity Contraction Theory in Shield Tunneling

The soil displacement and stress produced by the shield tail gap can be obtained by integrating the soil displacement generated from the gap per unit volume. As shown in Fig. 2, supposing that h represents the depth of tunnel centerline; g represents the gap thickness; the ground lose S is the gap between two connected circles with different radius ($S = S_1 - S_2$); $\varepsilon = S/S_1$ represents the ground loss ratio. It is noted that the depth and radius of the outer circle are h and R, and those of the inner circle are $h + g/2$ and $r = R - g/2$.

The gap parameter "g" was introduced by Lo and Rowe (1982), Rowe and Kack (1983) and Lee *et al.* (1992), to study the ground loss. Rowe and Kack (1983) defined the gap parameter g as the magnitude of the equivalent two-dimensional void formed around the tunnel due to the combined effects of the three-dimensional elastoplastic ground deformation at the tunnel face, overexcavation of soil around the periphery of the tunnel shield, and the physical gap that is related to the tunneling machine, shield, and lining geometry.

Loganathan and Poulos (1998) defined the equivalent ground

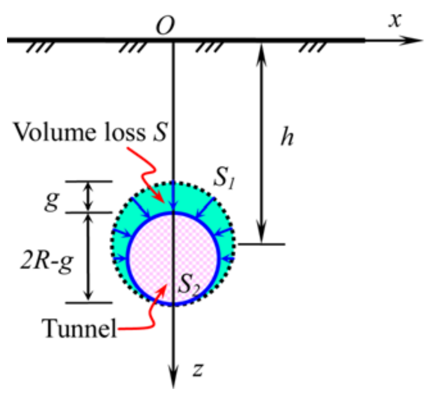

Fig. 2. Soil Displacement of Shield Tail Gap

loss and the relationship between the gap parameter and the equivalent ground loss.

The advantages in using the gap parameter to define the equivalent ground loss parameter are as follows: 1) The various construction methods and tunneling equipment configurations can be considered; and 2) elastoplastic behavior of the soil can be incorporated.

The undrained gap parameter "g" can be estimated as shown:

$$g = G_p + U^*_{3D} + \omega \tag{10}$$

where G_p is the physical gap between the liner and the perimeter of the excavation and includes the thickness of the TBM tailskin and the clearance required for erection of the liner; U^*_3D is a measure of the soil movements ahead of the face of the tunnel; and ω is the workmanship is a measure of the overcutting as the TBM is steered (Lee *et al.*, 1992, provide details on how to obtain each of the three components of the gap parameter).

The soil displacement components $U_x(x, z)$ and $U_z(x, z)$ generated by tunneling are deduced by integration:

$$\begin{aligned} U_x(x,z) &= \iint_S u_x(x,z)dS = \iint_{S_1-S_2} u_x(x,z)d\xi d\eta \\ &= \iint_{S_1} u_x(x,z)d\xi d\eta - \iint_{S_2} u_x(x,z)d\xi d\eta \\ &= \int_{h-R}^{h+R}\int_{-\sqrt{R^2-(\eta-h)^2}}^{\sqrt{R^2-(\eta-h)^2}} u_x(x,z)d\xi d\eta \\ &\quad - \int_{h-R+g}^{h+R}\int_{-\sqrt{\left(R-g/2\right)^2-\left(\eta-h-g/2\right)^2}}^{\sqrt{\left(R-g/2\right)^2-\left(\eta-h-g/2\right)^2}} u_x(x,z)d\xi d\eta \end{aligned} \tag{11}$$

$$\begin{aligned} U_z(x,z) &= \iint_S u_z(x,z)dS = \iint_{S_1-S_2} u_z(x,z)d\xi d\eta \\ &= \iint_{S_1} u_z(x,z)d\xi d\eta - \iint_{S_2} u_z(x,z)d\xi d\eta \\ &= \int_{h-R}^{h+R}\int_{-\sqrt{R^2-(\eta-h)^2}}^{\sqrt{R^2-(\eta-h)^2}} u_z(x,z)d\xi d\eta \\ &\quad - \int_{h-R+g}^{h+R}\int_{-\sqrt{\left(R-g/2\right)^2-\left(\eta-h-g/2\right)^2}}^{\sqrt{\left(R-g/2\right)^2-\left(\eta-h-g/2\right)^2}} u_z(x,z)d\xi d\eta \end{aligned} \tag{12}$$

where $u_x(x, z)$ and $u_z(x, z)$ can be expressed according to Eq. (8):

$$\left.\begin{aligned} u_x(x,z) &= -\frac{(x-\xi)}{2\pi}\left(\frac{1}{r_1^2}+\frac{1}{r_2^2}\right)+\frac{2z(x-\xi)(z+\eta)}{\pi r_2^4} \\ u_z(x,z) &= -\frac{1}{2\pi}\left(\frac{z-\eta}{r_1^2}-\frac{3z+\eta}{r_2^2}\right)-\frac{2z(x-\xi)^2}{\pi r_2^4} \end{aligned}\right\} \tag{13}$$

in which $r_1 = [(x-\xi)^2+(z-\eta)^2]^{1/2}$, $r_2 = [(x-\xi)^2+(z+\eta)^2]^{1/2}$.

2.2 Tunnel-Soil-Pile Interaction Mechanics on Kerr Foundation Model

2.2.1 Foundation Model

Figure 3 shows the tunnel-soil-pile models in the Winkle and Kerr foundation model. Among existing researches, the interaction analyses are commonly conducted based on the Winkler foundation model. The Winkler foundation model assumes that the soil can be simulated by non-connected discrete springs, as shown in Fig. 3(a). For the Winkler model, the interaction between the adjacent springs cannot be considered. Owing to the discontinuity of adjacent springs, the bending moments of piles are frequently overestimated by the Winkler-based solution. To overcome the above-mentioned disadvantages, Kerr (1965, 1985) improved the model with two spring layers and one shear layer to consider the connecting effects of distributed springs, as indicated in Fig. 3(b).

2.2.2 Horizontal Displacement Solution of Single Pile on Winkler Foundation Model

The tunnel-soil-pile interaction introduced by the Winkler model is indicated in Fig. 3(a). In the analyses process, the assumptions are set as: 1) the pile is regarded as a linear elastic foundation beam satisfying the Winkler foundation model; 2) surrounding soil is equivalent to a continuous homogeneous medium; and 3) the tunnel-soil-pile interaction is simulated with continuously distributed spring, and the pile is always in contact with the surrounding soil, which satisfies the deformation compatibility conditions.

Thus, the controlled equation for the effects of soil lateral displacement on the pile can be obtained:

$$\frac{d^4S_t(z)}{dz^4} + 4\lambda^4[S_t(z) - S_x(z)] = 0 \tag{14}$$

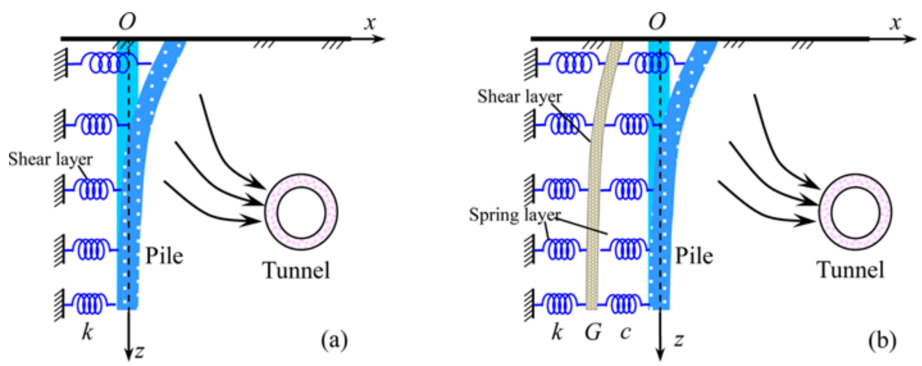

Fig. 3. Tunnel-Soil-Pile Interaction Model: (a) Winkler Type, (b) Kerr Type

where $S_t(z)$ is the pile horizontal displacement; $S_x(z)$ is the soil horizontal displacement in the free-field obtained by Eq. (11), and $\lambda = (k_z/4EI)^{1/4}$. k_z is the reaction force modulus of the surrounding soil defined as the ratio of soil resistance to pile deformation at arbitrary unit length of the pile, which is constant along the depth for homogeneous foundation. In this work, k_z is adopted based on the formula proposed by Vesic (1961) as:

$$k_z = \frac{0.65E_s}{D(1-v^2)}\sqrt[12]{\frac{D^4E_s}{EI}} \tag{15}$$

in which E_s denotes the elastic modulus of soil; D denotes the pile diameter; v represents the soil Poisson's ratio; and EI represents the pile bending stiffness.

The solution of the differential Eq. (14) is obtained as:

$$S_t(z) = C_1e^{\lambda z}\sin(\lambda z) + C_2e^{\lambda z}\cos(\lambda z) + C_3e^{-\lambda z}\sin(\lambda z) + C_4e^{-\lambda z}\cos(\lambda z) + S_t^*(z) \tag{16}$$

where $S_t^*(z)$ is the corresponding solution for $4\lambda^4S_x(z)$, which can be calculated by fitting the soil displacement with a cubic function and then substituting it into Eq. (14). C_1, C_2, C_3, C_4 are undetermined coefficients, which can be obtained by the pile boundary conditions. For the friction pile, the end of the pile is assumed completely free. For the end-bearing pile, the end of the pile is assumed completely fixed. It is presumed that the shear force and the moment are zero for the free pile top, while the slope and shear force at the pile top are zero for the non-rotating pile top.

Furthermore, the additional pile angle $\theta_t(z)$, bending moment $M_t(z)$ and shear force $Q_t(z)$ are derived as:

$$\begin{aligned}\theta_t(z) = \frac{dS_t(z)}{dz} = \lambda\{&C_1e^{\lambda z}[\sin(\lambda z)+\cos(\lambda z)] + \\ &C_2e^{\lambda z}[-\sin(\lambda z)+\cos(\lambda z)] + \\ &C_3e^{-\lambda z}[-\sin(\lambda z)+\cos(\lambda z)] + \\ &C_4e^{-\lambda z}[-\sin(\lambda z)-\cos(\lambda z)]\} + \frac{dS_t^*(z)}{dz}\end{aligned} \tag{17}$$

$$\begin{aligned}M_t(z) = -EI\frac{dS_t^{\,2}(z)}{dz^2} = 2\lambda^2EI[&C_1e^{\lambda z}\cos(\lambda z) - \\ &C_2e^{\lambda z}\sin(\lambda z) - C_3e^{-\lambda z}\cos(\lambda z) + \\ &C_4e^{-\lambda z}\sin(\lambda z) - EI\frac{dS_t^{*2}(z)}{dz^2}\end{aligned} \tag{18}$$

$$\begin{aligned}Q_t(z) = -EI\frac{dS_t^{\,3}(z)}{dz^3} = -2\lambda^3EI\{&C_1e^{\lambda z}[-\sin(\lambda z)+\cos(\lambda z)] + \\ &C_2e^{\lambda z}[-\sin(\lambda z)-\cos(\lambda z)] + \\ &C_3e^{-\lambda z}[\sin(\lambda z)+\cos(\lambda z)] + \\ &C_4e^{-\lambda z}[-\sin(\lambda z)+\cos(\lambda z)]\} - EI\frac{dS_t^{*3}(z)}{dz^3}\end{aligned} \tag{19}$$

2.2.3 Horizontal Displacement Solution of Single Pile on Kerr Foundation Model

The basic assumptions of the Kerr foundation model are as follows: 1) the pile is regarded as a cylindrical beam with a diameter of D and a stiffness of EI longitudinally; 2) the shear layer produces only shear deformation but no compression deformation; 3) no gap exists between the pile and the surrounding soil, and the pile deformation is coordinated with the foundation; and 4) no lateral friction exists between the pile and the foundation.

The incremental load $F(z)$ acting on the pile satisfies the following formula:

$$\left(1+\frac{k}{c}\right)F(z) - \frac{G}{c}F''(z) = kS_x(z) - GS_x''(z) \tag{20}$$

where $S_x(z)$ is the soil horizontal displacement in free-field caused by tunneling and can be obtained by Eq. (11); z is the depth below the ground surface; G represents the shear stiffness for the shear layer, which is given by:

$$G = \frac{E_st}{6(1+\nu)} \tag{21}$$

where E_s represents the soil elastic modulus; t denotes the thickness of the shear layer; c denotes the stiffness of the right-side spring of the shear layer, which is assumed as $c = nk$; n denotes the soil spring coefficient; k denotes the stiffness of the left-side spring of the shear layer, as:

$$k = \frac{0.65E_s}{t(1-\nu^2)}\sqrt[12]{\frac{D^4E_s}{EI}} \tag{22}$$

The incremental load on the pile can be deduced:

$$F(z) = \eta\left[\frac{nkS_x(z)}{n+1} - \frac{n^2GS_x''(z)}{(n+1)^2} - \sum_{i=2}^{\infty}\frac{n^2G^iS_x^{(2i)}(z)}{k^{i-1}(n+1)^{i+1}}\right] \tag{23}$$

where η is the load modification coefficient, from 0.4 to 1.0. Eliminating the high order approximation term in the above equation, the incremental load can be approximated:

$$F(z) = \eta\left[\frac{nk}{n+1}S_x(z) - \frac{n^2G}{(n+1)^2}S_x''(z)\right] \tag{24}$$

Under this load, the deflection of the pile can be assumed as:

$$u_s(x) = u_{s1}(x) + u_{s2}(x) \tag{25}$$

where u_{s1} and u_{s2} represent the deformation of right-side spring and shear layer, respectively. Supposing the stress on the left-side of the pile is f_1 and that on the left-side of the shear layer is f_2:

$$f_1(z) = cu_{s1}(x) = c[u_s(x) - u_{s2}(x)] \tag{26}$$

$$f_2(z) = ku_{s2}(x) \tag{27}$$

For the shear layer, it can be expressed as:

$$f_2(z) = -G\frac{d^2u_{s2}(x)}{dz^2} + ku_{s2}(x) \tag{28}$$

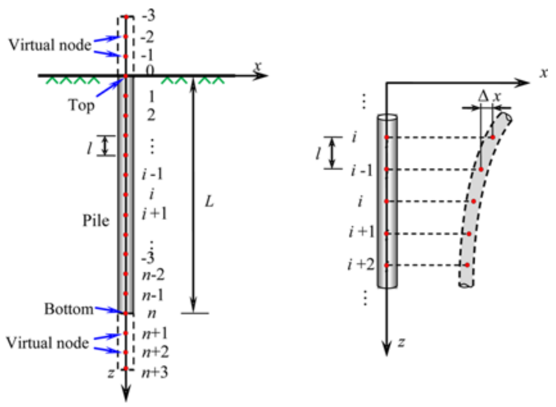

Fig. 4. Finite Difference Element Discreteness of Pile

The pile horizontal displacement can be deduced:

$$u_s(x) = \left(1 + \frac{k}{c}\right) u_{s2}(x) - \frac{G}{c}\frac{d^2 u_{s2}(x)}{dz^2} \tag{29}$$

The equilibrium differential equation for the pile under loading is given by:

$$EI\frac{d^4 u_s(x)}{dz^4} + f_1(z)D = F(z)D \tag{30}$$

Through simultaneous formulas above, the final equation is obtained as follows:

$$-\frac{EIG}{Dc}\frac{d^6 u_{s2}}{dz^6} + \frac{EI(c+k)}{Dc}\frac{d^4 u_{s2}}{dz^4} - G\frac{d^2 u_{s2}}{dz^2} + ku_{s2} = F \tag{31}$$

After obtaining the horizontal displacement of the shear layer $\{u_{s2}\}$, that of a single pile $\{u_s\}$ can be solved according to Eq. (29). It is noted that when c of Eq. (31) is infinite, the model degrades to Pasternak foundation model.

Equation (31) is a sixth-order differential equation. Thus, it is complex to obtain the corresponding analytical solution. The finite differential method therefore is applied in this study. Fig. 4 illustrates the discreteness of a pile, which can be divided into n elements with length $l = L/n$. L is the pile length. The elements are numbered successively from the top to the end as 0, 1, …, n–1, n. To facilitate the differential operation, six virtual elements are increased at the two ends of the pile (node –3, –2, –1 and $n+1$, $n+2$, $n+3$).

Taking a standard node i as an example, the following relationship between the derivative and the difference in the central differential format is obtained:

$$\left(\frac{du_{s2}}{dz}\right)_i = \frac{(u_{s2})_{i+1} - (u_{s2})_{i-1}}{2l} \tag{32a}$$

$$\left(\frac{d^2u_{s2}}{dz^2}\right)_i = \frac{(u_{s2})_{i+1} - 2(u_{s2})_i + (u_{s2})_{i-1}}{l^2} \tag{32b}$$

$$\left(\frac{d^3u_{s2}}{dz^3}\right)_i = \frac{(u_{s2})_{i+2} - 2(u_{s2})_{i+1} + 2(u_{s2})_{i-1} - (u_{s2})_{i-2}}{2l^3} \tag{32c}$$

$$\left(\frac{d^4u_{s2}}{dz^4}\right)_i = \frac{(u_{s2})_{i+2} - 4(u_{s2})_{i+1} + 6(u_{s2})_i - 4(u_{s2})_{i-1} + (u_{s2})_{i-2}}{l^4} \tag{32d}$$

$$\left(\frac{d^5u_{s2}}{dz^5}\right)_i = \frac{\begin{array}{c}(u_{s2})_{i+3} - 5(u_{s2})_{i+2} + 7(u_{s2})_{i+1} - 7(u_{s2})_{i-1} \\ +5(u_{s2})_{i-2} - (u_{s2})_{i-3}\end{array}}{2l^5} \tag{32e}$$

$$\left(\frac{d^6u_{s2}}{dz^6}\right)_i = \frac{\begin{array}{c}(u_{s2})_{i+3} - 6(u_{s2})_{i+2} + 15(u_{s2})_{i+1} - 20(u_{s2})_i \\ +15(u_{s2})_{i-1} - 6(u_{s2})_{i-2} + (u_{s2})_{i-3}\end{array}}{l^6} \tag{32f}$$

Regarding the Eq. (20), a relevant finite differential form can be reached through discrete methods:

$$\begin{aligned}
&-\frac{EIG}{Dcl^6}(u_{s2})_{i-3} + \left(\frac{6EIG}{Dcl^6} + \frac{EI(c+k)}{Dcl^4}\right)(u_{s2})_{i-2} \\
&+\left(-\frac{15EIG}{Dcl^6} - 4\frac{EI(c+k)}{Dcl^4} - \frac{G}{l^2}\right)(u_{s2})_{i-1} \\
&+\left(\frac{20EIG}{Dcl^6} + 6\frac{EI(c+k)}{Dcl^4} + 2\frac{G}{l^2} + k\right)(u_{s2})_i \\
&+\left(-\frac{15EIG}{Dcl^6} - 4\frac{EI(c+k)}{Dcl^4} - \frac{G}{l^2}\right)(u_{s2})_{i+1} \\
&+\left(\frac{6EIG}{Dcl^6} + \frac{EI(c+k)}{Dcl^4}\right)(u_{s2})_{i+2} - \frac{EIG}{Dcl^6}(u_{s2})_{i+3} = F_i
\end{aligned} \tag{33}$$

The deflection, rotation, moment, and shear force of the pile are as follows:

$$\begin{aligned}
u_{si} &= \left(1+\frac{k}{c}\right)(u_{s2})_i - \frac{G}{c}\left(\frac{d^2u_{s2}}{dz^2}\right)_i = -\frac{G}{cl^2}(u_{s2})_{i-1} \\
&\quad + \left(\frac{c+k}{c} + \frac{2G}{cl^2}\right)(u_{s2})_i - \frac{G}{cl^2}(u_{s2})_{i+1}
\end{aligned} \tag{34a}$$

$$\begin{aligned}
\theta_i &= \left(\frac{du_s}{dz}\right)_i = \left(1+\frac{k}{c}\right)\left(\frac{du_{s2}}{dz}\right)_i - \frac{G}{c}\left(\frac{d^3u_{s2}}{dz^3}\right)_i \\
&= \frac{G}{2cl^3}(u_{s2})_{i-2} + \left(-\frac{c+k}{2cl} - \frac{G}{cl^3}\right)(u_{s2})_{i-1} \\
&\quad + \left(\frac{c+k}{2cl} + \frac{G}{cl^3}\right)(u_{s2})_{i+1} - \frac{G}{2cl^3}(u_{s2})_{i+2}
\end{aligned} \tag{34b}$$

$$\begin{aligned}
M_i &= EI\left(\frac{d^2u_s}{dz^2}\right)_i = EI\left[\left(1+\frac{k}{c}\right)\left(\frac{d^2u_{s2}}{dz^2}\right)_i - \frac{G}{c}\left(\frac{d^4u_{s2}}{dz^4}\right)_i\right] \\
&= EI\left\{-\frac{G}{cl^4}(u_{s2})_{i-2} + \left(\frac{c+k}{cl^2} + \frac{4G}{cl^4}\right)(u_{s2})_{i-1}\right. \\
&\quad + \left(-\frac{2(c+k)}{cl^2} - \frac{6G}{cl^4}\right)(u_{s2})_i \\
&\quad \left. + \left(\frac{c+k}{cl^2} + \frac{4G}{cl^4}\right)(u_{s2})_{i+1} - \frac{G}{cl^4}(u_{s2})_{i+2}\right\}
\end{aligned} \tag{34c}$$

$$\begin{aligned}
Q_i &= EI\left(\frac{d^3u_s}{dz^3}\right)_i = EI\left[\left(1+\frac{k}{c}\right)\left(\frac{d^3u_{s2}}{dz^3}\right)_i - \frac{G}{c}\left(\frac{d^5u_{s2}}{dz^5}\right)_i\right] \\
&= EI\left\{\frac{G}{2cl^5}(u_{s2})_{i-3} + \left(-\frac{(c+k)}{2cl^3} - \frac{5G}{2cl^5}\right)(u_{s2})_{i-2}\right. \\
&\quad + \left(\frac{(c+k)}{cl^3} + \frac{7G}{2cl^5}\right)(u_{s2})_{i-1} + \left(-\frac{(c+k)}{cl^3} - \frac{7G}{2cl^5}\right)(u_{s2})_{i+1} \\
&\quad \left. + \left(\frac{(c+k)}{2cl^3} + \frac{5G}{2cl^5}\right)(u_{s2})_{i+2} - \frac{G}{2cl^5}(u_{s2})_{i+3}\right\}
\end{aligned} \tag{34d}$$

The pile top is supposed to be free with the pile end fixed. Thus, the boundary conditions can be given: both the moment and shear force are not induced at the pile top ($z \to 0$); and both the deflection and rotation do not exist at the pile end ($z \to H$). In addition to considering these boundary conditions, two boundary conditions are necessary to be increased for the shear layer: the internal force of the shear layer is none at the top ($z \to 0$); and the shear deformation and rotation of the shear layer are zero at the pile end ($z \to H$):

$$\left(\frac{d^2u_{s2}}{dz^2}\right)_0 = \frac{(u_{s2})_1 - 2(u_{s2})_0 + (u_{s2})_{-1}}{l^2} = 0 \tag{35a}$$

$$(u_{s2})_{n+1} = 0 \tag{35b}$$

According to the boundary conditions, the virtual node is eliminated and the displacement equation of the shear layer is obtained:

$$\{u_s\} = [K]^{-1} \cdot \{F\} \tag{36}$$

where $\{u_s\} = \left[(u_{s2})_0, (u_{s2})_1, \cdots, (u_{s2})_n\right]^T$; the incremental loading on the pile top $\{F\} = \left[F_0, F_1, F_2, \cdots F_n\right]^T$; and soil horizontal stiffness matrix $[K]$ can be expressed as:

$$[K] = \begin{bmatrix} \delta+2\gamma+4\beta-8\alpha & -4\beta-10\alpha & 2\beta+2\alpha & 2\alpha & & & & & \\ \gamma+2\beta+6\alpha & \delta-\beta-2\alpha & \gamma-\alpha & \beta & \alpha & & & & \\ \beta-2\alpha & \gamma-\alpha & \delta & \gamma & \beta & \alpha & & & \\ \alpha & \beta & \gamma & \delta & \gamma & \beta & \alpha & & \\ & \ddots & \ddots & \ddots & \ddots & \ddots & \ddots & \ddots & \\ & & \alpha & \beta & \gamma & \delta & \gamma & \beta & \alpha \\ & & & \alpha & \beta & \gamma & \delta & \gamma & \beta \\ & & & & \alpha & \beta & \gamma & \delta & \gamma-\alpha \\ & & & & & \alpha & \beta & \gamma+\alpha & \delta+\beta+8\alpha \end{bmatrix} \tag{37}$$

According to Eq. (24), the load can be expressed as a finite differential form through discrete methods:

$$\begin{aligned} F_i &= \frac{nk}{n+1}(S_x)_i - \frac{n^2G}{(n+1)^2}\frac{(S_x)_{i+1} - 2(S_x)_i + (S_x)_{i-1}}{l^2} \\ &= -\frac{n^2G}{l^2(n+1)^2}(S_x)_{i+1} + \left(\frac{nk}{n+1} + \frac{2n^2G}{l^2(n+1)^2}\right)(S_x)_i \\ &\quad -\frac{n^2G}{l^2(n+1)^2}(S_x)_{i-1} \end{aligned} \tag{38}$$

After obtaining $(u_{s2})_i$, the pile horizontal displacement can be solved according to Eq. (29):

$$\begin{aligned} u_{si} &= \left(1 + \frac{k}{c}\right)(u_{s2})_i - \frac{G}{c}\left(\frac{d^2u_{s2}}{dz^2}\right)_i \\ &= -\frac{G}{cl^2}(u_{s2})_{i-1} + \left(\frac{c+k}{c} + \frac{2G}{cl^2}\right)(u_{s2})_i - \frac{G}{cl^2}(u_{s2})_{i+1} \end{aligned} \tag{39}$$

Consequently, the pile bending moment can be obtained:

$$M_i = EI\left(\frac{d^2u_s}{dz^2}\right)_i = \frac{EI}{l^2}\left[(u_s)_{i+1} - 2(u_s)_i + (u_s)_{i-1}\right] \tag{40}$$

3. Verification

3.1 Analyses of Free-Field Displacement

3.1.1 Case 1

The field measurement and the study of Loganathan and Poulos (1998) have been selected to validate the solution for the free-field soil displacement according to the cylindrical cavity contraction method discussed above. As shown in Fig. 5, the concerned parameters are set as follows: a tunnel diameter of 8.5 m, stiff London clay with an elastic modulus of 35 MPa and a unit weight of 19 kN/m^3, a gap parameter of 58 mm. Moreover, the free-field horizontal displacement is calculated at the vertical line which maintains a distance of 6 m from the ground surface

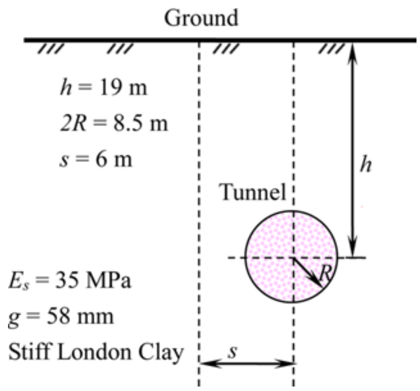

Fig. 5. Case 1 of Free-Field Displacement Analyses

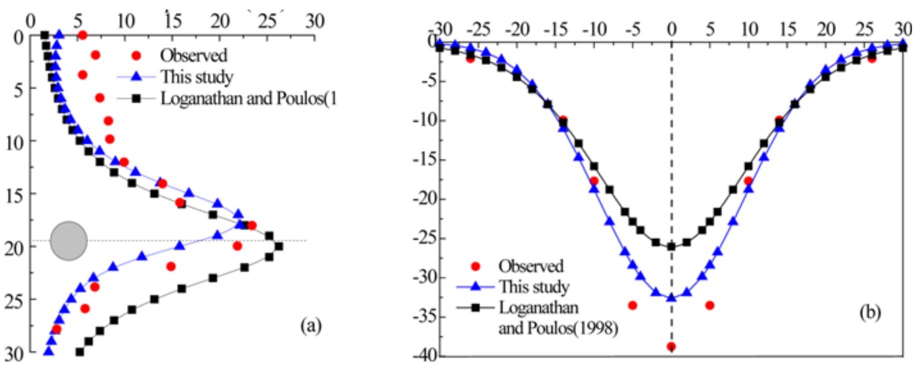

Fig. 6. Comparison of Free-Soil Displacement of Case 1: (a) Horizontal Displacement, (b) Surface Settlement

to the tunnel centerline. The free-field displacement solved by the cylindrical cavity contraction method is given as Eqs. (11) and (12).

It can be observed in Fig. 6(a) that good agreements are obtained by the two above-mentioned approaches, while the results obtained by the cylindrical cavity contraction theory are more accurate to the monitoring data. It is noted that the surface subsidence trends through both the cylindrical cavity contraction theory and that of Loganathan and Poulos (1998) are highly similar, which present a trough-shape as shown in Fig. 6(b). In particular, the results through the analytical method proposed in this paper is closer to the actual engineering data, which is also more accurate than Loganathan and Poulos (1998).

3.1.2 Case 2

A second case is selected to verify the free-field displacement behavior obtained by the cavity contraction theory through comparing with the field measurements and the analytical prediction of Loganathan and Poulos (1998). The Bangkok tunnel maintains a depth of 18 m and an outer diameter of 2.66 m, while the elastic modulus and the unit weight of the soft clay is given as 20 MPa and 17 kN/m^{3,} respectively. The gap parameter is 81 mm, and the section of horizontal displacement is 4 m away from the tunnel centerline (see Fig. 7).

It can be revealed from Figs. 8(a) and 8(b) that deformation trends predicted by two solution show reasonable alignments, however, more resemblance is gained between the proposed analytical approach and the measured data, regarding the pile horizontal displacement and surface subsidence. It can be concluded that the solution presented in this work achieves more accuracy.

3.2 Analyses of Pile Response

3.2.1 Case 1

Full-scale case researches were reported by Lee *et al.* (1994), analyzing the pile horizontal displacement induced by the construction of tunneling (see Fig. 9). The case involves the tunneling for the Angel Underground Station in London. The pile maintains a length of 28 m, a diameter of 1.2 m and a modulus of 30 GPa. The spacing between the tunnel centerline and the pile centerline is 5.7 m, and the tunnel depth is 15 m. The tunneling process is divided into two stages: a pilot tunnel of a diameter of 4.5 m first and then an enlargement of an outer diameter of 8.25 m. Observed ground loss ratio for the pilot tunnel is approximately 1.5%, while that for the enlargement is 0.5%. The soil is assumed to be homogeneous with an equivalent elastic modulus of 54 MPa, of which the cohesion is $C = 15$ kPa, the critical friction angle is $\varphi_{cv} = 25°$, the unit weight is $\gamma_w = 18$ kN/m, the relative density is $I_d = 0.8$, the lateral pressure coefficient is $K_0 = 0.5$ and the Poisson ratio is $\nu = 0.2$.

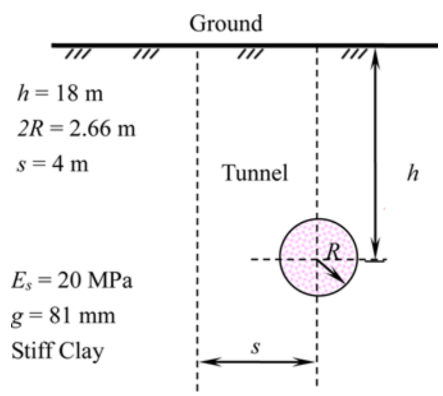

Fig. 7. Case 2 of Free-Field Displacement Analyses

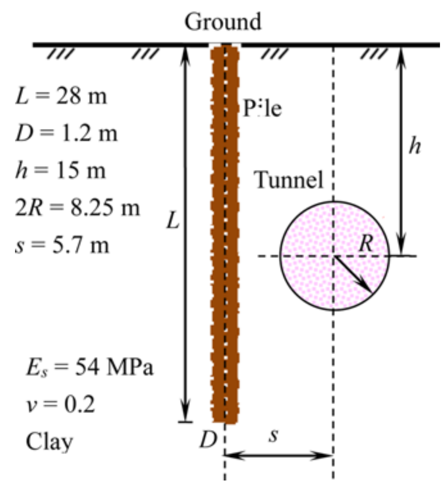

Fig. 9. Case 1 of Pile Response Analyses

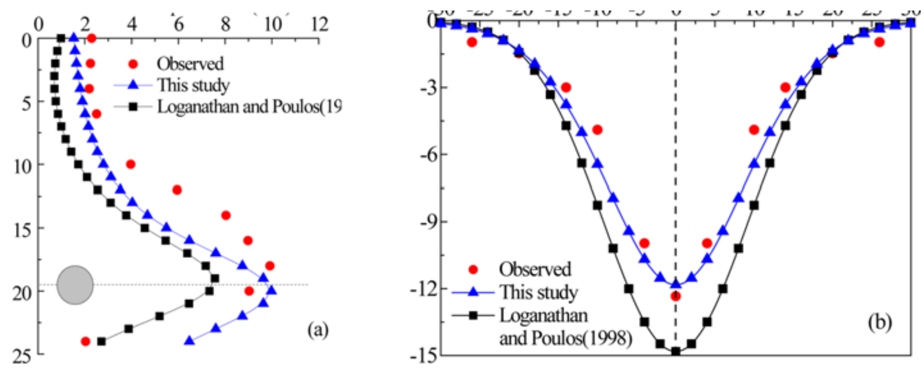

Fig. 8. Comparison of Free-Soil Displacement of Case 2: (a) Horizontal Displacement, (b) Surface Settlement

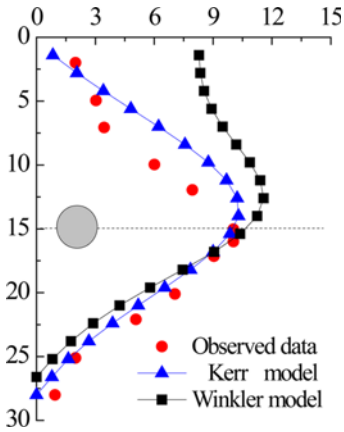

Fig. 10. Comparison of Pile Horizontal Displacement of Case 1

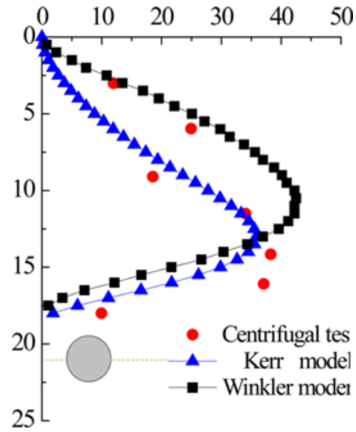

Fig. 12. Comparison of Pile Bending Moment of Case 2

The comparisons of pile horizontal displacement obtained in this study on the basis of the Kerr foundation model and Winkler model are shown in Fig. 10. The observed data is also listed for comparative analysis in this figure. It is evident that the observed data and the predicted results through two foundation models are in good agreement below the tunnel centerline, nevertheless, the proposed analytical methods overpredict the horizontal displacement above the tunnel centerline, especially for the Winkler model. The maximum occurs just above the tunnel centerline, which receives an overprediction of 11.1 mm compared with the Kerr-based solution and 10.1 mm with the measured data (an approximated difference of 10%). It is proved that the Kerr foundation model that takes account of the soil shear effects preferably coincides with the engineering practice better.

3.2.2 Case 2

Centrifuge tests were performed by Loganathan *et al.* (2000), observing the pile response induced by tunneling in Kaolin clay. The pile adopted aluminum alloy hollow tube and the test was conducted at an acceleration of 100 g. Converted into the prototype (see Fig. 11), the distance between the tunnel (6 m in diameter, 21 m in depth and 1% in the average ground loss ratio) and the pile (18 m in length, and 0.8 m in diameter) is 5.5 m. Considering the epoxy coated on tested pile, the effective pile diameter is selected as 0.9 m, and the elastic modulus of pile is 20.5 GPa. The soil has an elastic modulus of 30 MPa, a cohesion and critical friction angle of $C = 20$ kPa and $\varphi_{cv} = 30°$, respectively. Moreover, its unit weight is $\gamma_w = 18.5$ kN/m^3; the relative density is $I_d = 0.9$; the lateral pressure coefficient is $K_0 = 0.5$; and the Poisson ratio is $\nu = 0.2$.

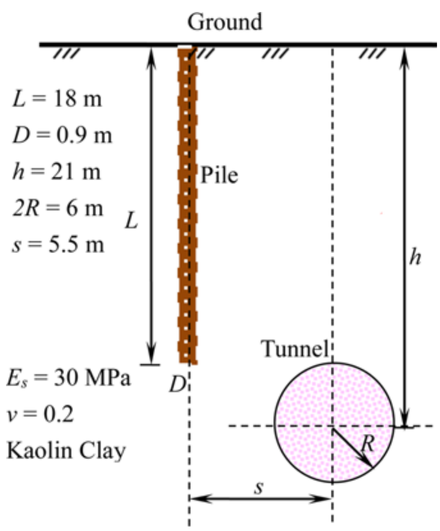

Fig. 11. Case 2 of Pile Response Analyses

The comparisons of pile bending moments calculated by the proposed solutions and the centrifuge test data are demonstrated in Fig. 12. The predicted trends using the Kerr foundation model and measured profiles have good consistencies even if the maximum bending moments, which occur at 13 m depth approximately, are underpredicted through the proposed solution. However, the bending moment calculated by the Winkler foundation model shows poor agreement with the centrifuge test data.

3.2.3 Case 3

Mu *et al.* (2012) presented the pile responses of a pile closely spaced to the tunnel construction through the displacement controlled finite element method (DCFEM). For the concerned parameters, the pile diameter is 0.8 m, the pile length is 25 m and

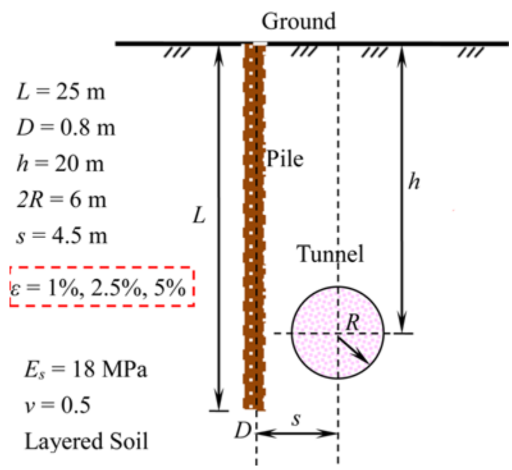

Fig. 13. Case 3 of Pile Response Analyses

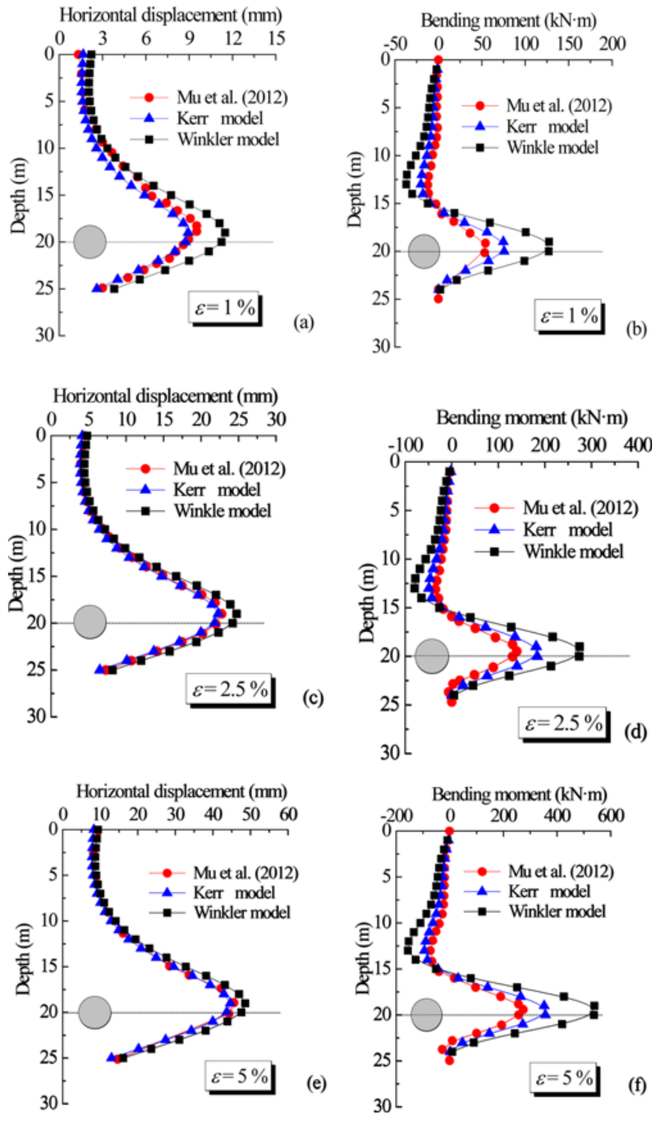

Fig. 14. Comparison of Pile Response of Case 3: (a) Horizontal Displacement (ε = 1%), (b) Bending Moment (ε = 1%), (c) Horizontal Displacement (ε = 2.5%), (d) Bending Moment (ε = 2.5%), (e) Horizontal Displacement (ε = 5%), (f) Bending Moment (ε = 5%)

the pile elastic modulus is 10 GPa (see Fig. 13). In addition, the tunnel with a diameter of 6 m and a buried depth of 20 m is 4.5 m away from the pile centerline. The soil is divided into two layers in the finite element: the upper soil is 10 m in thickness, and the elastic modulus and the Poisson's ratio of soil are 12 MPa and 0.5, respectively; the soil elastic modulus of the lower layer is 24 MPa, with a Poisson's ratio of 0.5. To simplify the calculation, the soil is supposed to be homogeneous with an equivalent elastic modulus of 18 MPa. Moreover, the soil cohesion is C = 15 kPa, the critical friction angle is φ_{cv} = 30°, the unit weight is γ_w = 18 kN/m^3, the relative density is I_d = 0.8, the lateral pressure coefficient is K_0 = 0.5 and Poisson ratio is ν = 0.5.

As shown in Fig. 14, the comparisons of pile horizontal displacement and bending moment predicted by the proposed methods on the basis of the Winkler model and Kerr foundation model are obtained along with those resulting from DCFEM, in which the ground loss ratio is 1%, 2.5% and 5%. It can be implicated that the predicted pile deformation based on the Kerr model is slightly smaller than the DCFEM, still similar to a certain degree. In additional, the maximum horizontal displacement occurs slightly above the tunnel centerline. In the case of ε=1%, the maximum value by DCFEM is 9.52 mm, overpredicted by 6.2% compared with that of the Kerr-based analytical solution, which is 8.93 mm. However, the Winkler-based horizontal displacement and the result from DCFEM show good agreements, expect at the tunnel centerline, where the Winkler-based solution overpredicts by 20.7%. When ε = 2.5%, the maximum value by DCFEM is 22.76 mm, about 1.9% over the Kerr-based solution and 8.7% under the Winkler-based solution; and when ε = 5%, the maximum value by DCFEM is 45.61 mm, about 2.1% over the Kerr-based solution and 6.6% under the Winkler-based solution. It is pronounced that the pile horizontal displacement predicted by the Kerr foundation model achieves better coincidence with the numerical simulation compared to the Winkler solution. It should be noticed that the distribution trend of the calculated and measured pile bending moment have a certain consistency. The pile bending moment based on the Kerr model is more resembling with that according to DCFEM.

4. Parameters Analyses

4.1 Influence of Soil Spring Coefficient *n* in Kerr Foundation

In view of the soil spring coefficient c (c = nk) as an additional term in Kerr foundation model, the value of n will affect the accuracy of the calculation results theoretically (see Fig. 15). The diameter, length and elastic modulus of the pile are set as 1.0 m, 30 m and 30 GPa, respectively. The centerline of the tunnel with a diameter of 6 m is buried at 18 m and 5.5 m away from the pile centerline. The average ground loss ratio is 4.0%. The soil elastic modulus is 30 MPa and the soil Poisson's ratio is 0.5. The shear layer thicknesses t is set as 1 m, 5 m, 8 m, 10 m and infinity, and the pile boundary condition are assumed to be free at the top and fixed at the end.

Figure 16 shows the influence of soil spring coefficient n on

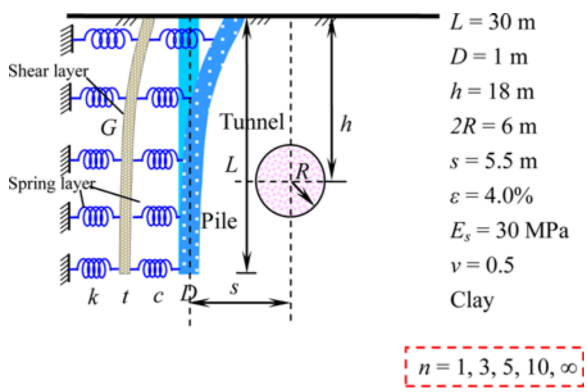

Fig. 15. Analyses Model of Soil Spring Coefficient *n*

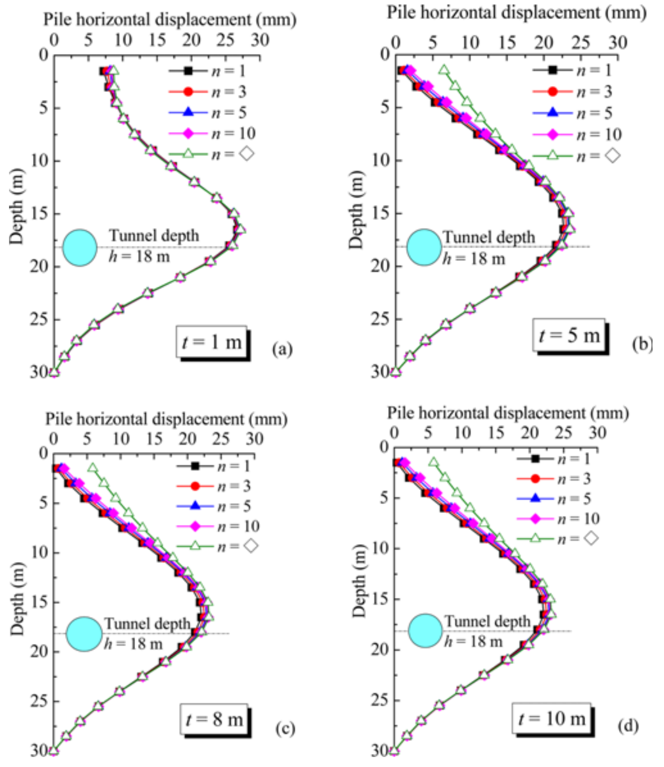

Fig. 16. Influence of Parameter n on Pile Horizontal Displacement: (a) t = 1 m, (b) t = 5 m, (c) t = 8 m, (d) t = 10 m

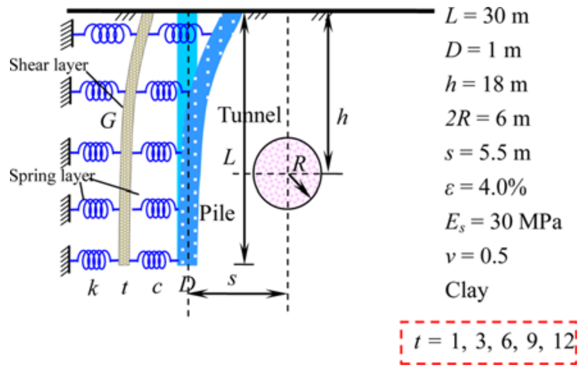

Fig. 17. Analyses Model of Shear Layer Thickness t

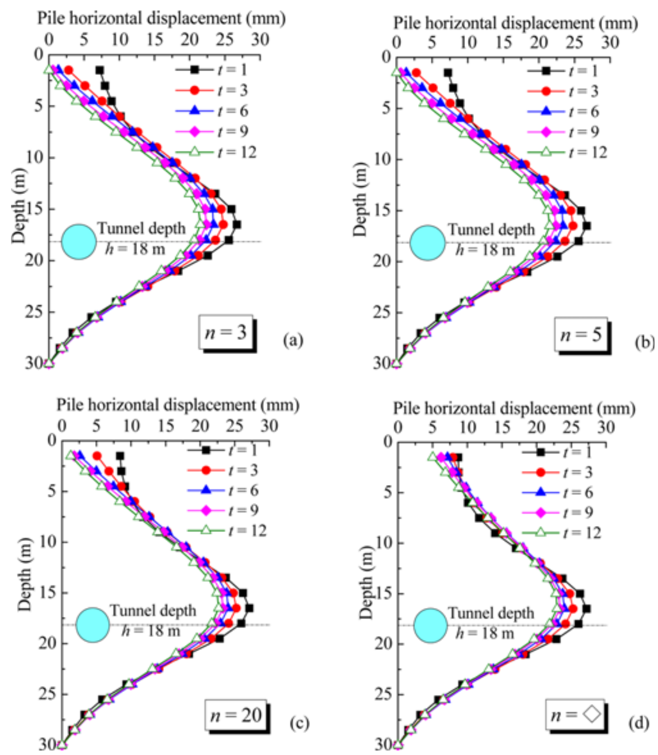

Fig. 18. Influence of Parameter t on Pile Horizontal Displacement: (a) n = 3, (b) n = 5, (c) n = 20, (d) n = ∞

the pile horizontal displacement in different shear layer thicknesses. As shown in the figure, the effects on the pile is mainly reflected nearby the pile head, while the displacement near the pile tip is almost negligible. The results are related to the pile boundary conditions, in which the fixed boundary condition restrains the displacement of the pile end, while the pile top adopts a free condition, resulting in the horizontal displacement varies with the coefficient n. By the addition of n value, a weak trend of increasing horizontal displacement at the top is observed. When the coefficient n is set as infinite, the model can be degenerated into the Pasternak foundation model.

4.2 Influence of Shear Layer Thickness t in Kerr Foundation

It is assumed in Fig. 17 that the pile diameter is 1.0 m, the length, 30 m, the elastic modulus, 30 GPa. The tunnel diameter is 6 m, the axis depth, 18 m. The average ground loss ratio is set as 4.0%. The centerline of the tunnel is 5.5 m away from the pile centerline. The soil elastic modulus is 30 MPa and the soil Poisson's ratio is 0.5. The soil spring coefficient n is set as 3, 5, 20 and infinity, and the pile boundary condition is assumed to be free at the top and fixed at the end.

Figure 18 shows the variations of pile horizontal displacement with different foundation shear layer thicknesses in the case of n = 3, 5, 20, and ∞. It is observed that the effect of t on the pile horizontal displacement mainly occurs above the centerline of tunnel, but there is little effect on the pile below the tunnel centerline. The significant effect of t on the horizontal displacement of pile takes place, that is, the displacement at the tunnel centerline is maximum and decreases with an increase in the thickness t. When the parameter t is set as zero, the model can be degenerated into the Winkler foundation model.

4.3 Influence of Pile Diameter D

It is assumed in Fig. 19 that the tunnel diameter is 6.4 m, the axis depth, 20 m. The average ground loss ratio is 2.0%. The tunnel centerline is 8 m away from the pile centerline. The pile length is 30 m, the elastic modulus, 30 GPa. The soil elastic modulus is 30 MPa and the soil Poisson's ratio is 0.4. The simplified analytical method proposed in this paper is adopted, in which the shear layer thicknesses t is set as 5, 10, 15 and 20 m, and the diameter is set as 0.6, 0.8, 1.0, 1.2, and 1.5 m.

Figure 20 indicates the pile horizontal deformation with the

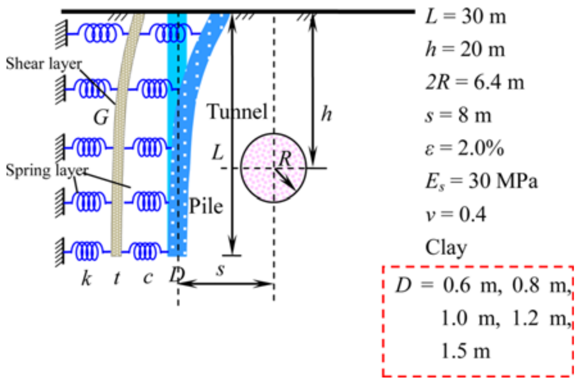

Fig. 19. Analyses Model of Pile Diameter D

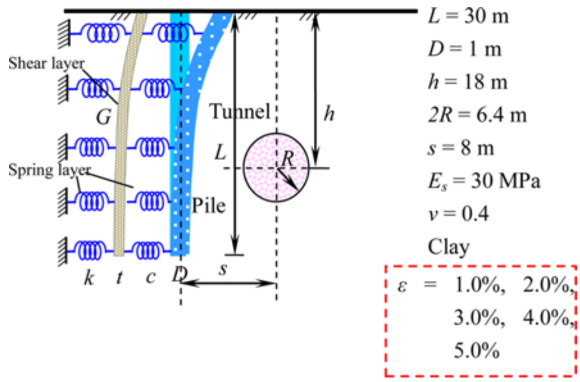

Fig. 21. Analyses Model of Ground Loss Ratio ε

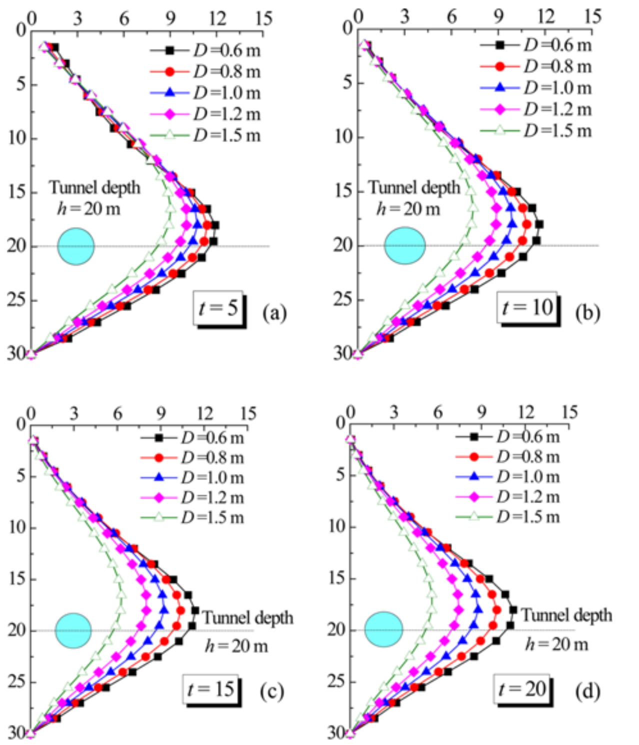

Fig. 20. Influence of Pile Diameter on Pile Horizontal Displacement: (a) t = 5, (b) t = 10, (c) t = 15, (d) t = 20

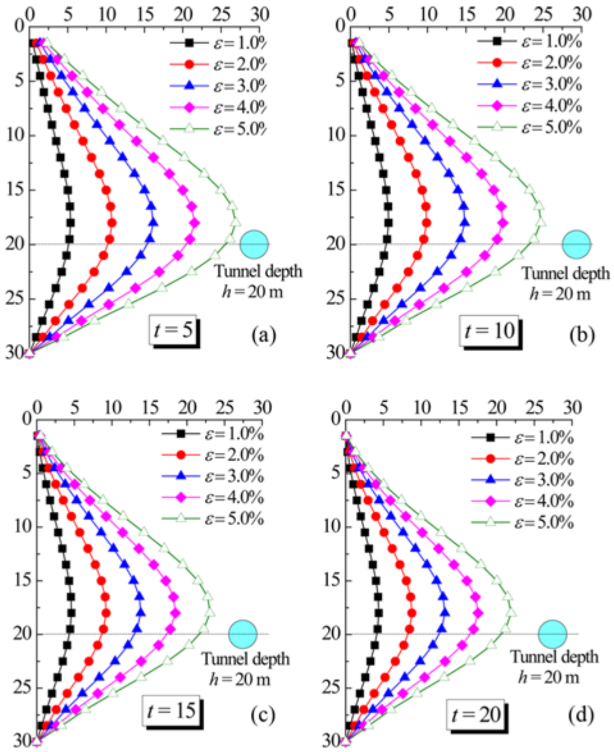

Fig. 22. Influence of Ground Loss Ratio on Pile Horizontal Displacement: (a) t = 5, (b) t = 10, (c) t = 15, (d) t = 20

response of the pile diameter. As can be seen, on condition of the same shear layer thickness, the larger the pile diameter, the smaller the pile horizontal displacement caused by tunnel excavation, resulting from the increasing of the pile bending stiffness EI with the increase of the diameter. The pile horizontal displacement is gradually reduced with the increase of the thickness of the shear layer in the case that the pile diameter maintains unchanged.

4.4 Influence of Ground Loss Ratio ε

It is assumed in Fig. 21 that the diameter of a pile is 1.0 m, with a length of 30 m, an elastic modulus of 30 GPa. The tunnel diameter is 6.4 m, and the buried depth is 20 m. The average ground loss ratio is set as 1.0%, 2.0%, 3.0%, 4.0%, and 5.0%. The centerline of the tunnel is 8 m away from the pile centerline. The soil elastic modulus is 30 MPa and the soil Poisson's ratio is 0.4. The shear layer thicknesses t is set as 5, 10, 15 and 20 m.

Figure 22 shows the horizontal displacement of adjacent single pile resulting from tunneling in different ground loss ratio. It is demonstrated that the horizontal deformation increases along with the pile ground loss ratio ε increasing. However, the pile horizontal displacement is inversely proportional to the shear layer thickness t when the ground loss ratio ε is unchanged.

4.5 Influence of Tunnel-pile Distance s

It is assumed in Fig. 23 that the pile diameter is 1.0 m, with a length of 30 m and an elastic modulus of 30 GPa. The tunnel diameter is 6.4 m, the buried depth is 20 m. The average ground loss ratio is 2.0%. The distance between the tunnel centerline and pile is set as 4, 6, 8, 10 and 20 m, respectively. The soil elastic

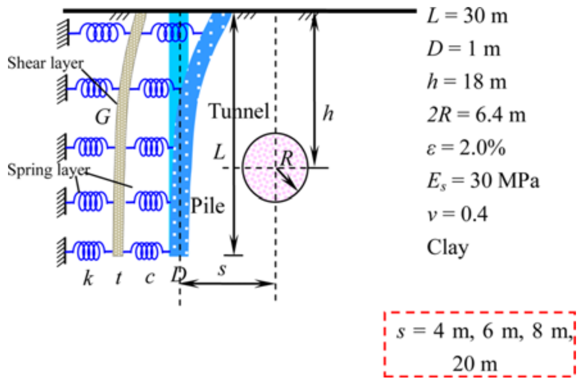

Fig. 23. Analyses Model of Tunnel-Pile Distance s

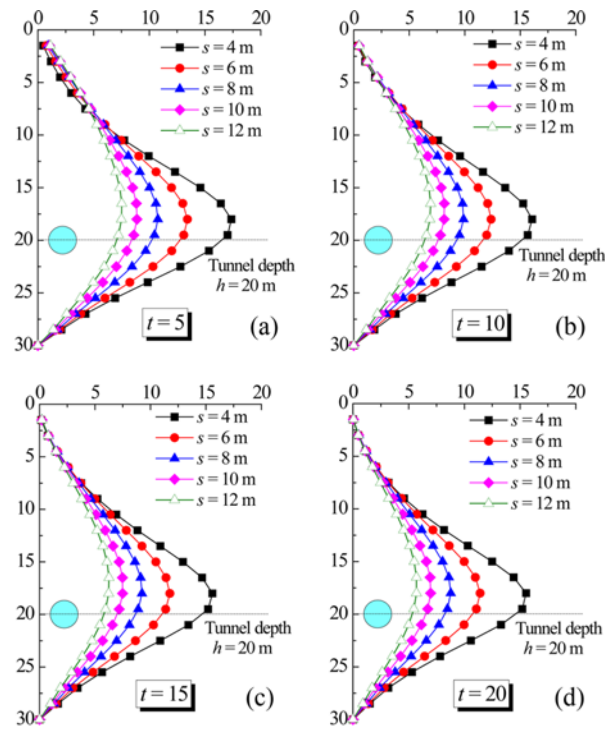

Fig. 24. Influence of Tunnel-Pile Distance on Pile Horizontal Displacement: (a) t = 5, (b) t = 10, (c) t = 15, (d) t = 20

modulus is 30 MPa and the soil Poisson's ratio is 0.4. The shear layer thickness t is set as 5, 10, 15 and 20 m.

Figure 24 shows the variety of the pile horizontal displacement influenced by the tunnel-pile distance. The results indicate that the maximum pile displacement, locating above the tunnel centerline, is inversely proportional to the tunnel-pile distance with the shear layer thickness unchanging. In addition, the horizontal deformation at the top of the pile increases slightly with the reduction of the tunnel-pile distance.

5. Conclusions

A simplified two-stage solution has been presented to the prediction for the pile deformation induced by soil displacement due to tunneling in clay. The pile response based on the Kerr foundation model is acquired by the free-field displacement solved by the cavity contraction theory. The presented solution is checked by comparisons with the existing results from DCFEM, the centrifuge modeling tests, and the field data, which obtains good agreements. It is proved that the cavity contraction theory is more accurate compared with the Loganathan and Poulos (1998) solution, and the Kerr foundation model considering the soil shear effects is reliable and servable to engineering practice.

The parametric analysis for the shear layer thickness t and the soil spring coefficient n of the Kerr foundation model is carried out for the pile horizontal displacement. It is observed that with the increasing of n, the pile horizontal deformation gradually increases with a relatively slow variation. When the soil spring coefficient n tends to infinity, the foundation model will degenerate to Pasternak foundation model. The shear layer thickness t is in inverse proportion to pile horizontal displacement. It approaches to the Winkler foundation model when t is small, which means the soil shear layer is thin. When the shear layer thickness t is zero, the foundation model will degenerate to Winkler foundation model. The calculation results show that the pile diameter D, the ground loss ratio ε and the tunnel-pile space s have significant effects on the pile horizontal deformation. When the soil spring coefficient n and the shear layer thickness t of the Kerr foundation model are constant, D and s are in inverse proportion to pile displacement, while ε is in direct proportion to pile displacement.

It is worth noting that the presented method is mainly limited to the simplified assumption of elastic and linear material. According to a given free-field deformation, any soil elasto-plasticity or nonlinearity, whether owing to interaction between the tunnel and the pile or soil shearing induced by tunneling, may emerge the maximum bending moments for the pile. Progressive mechanics such as the relative uplift failure and the gap between the soil and the pile, advanced elasto-plastic or elasto-viscoplastic constitutive models for the soil, should be introduced into this study. The suggested methods cannot take into consideration for the influence of pile joints permitting rotation or axial movements and the pile group effect. Therefore, further researches on these subjects are still necessary so as to more accurately estimate the tunnel-soil-pile interaction problem.

Acknowledgements

The authors acknowledge the financial support provided by Natural Science Foundation of China (No. 41772331), and by Project Program of State Key Laboratory of Track Technology of High-Speed Railway (No. 2018YJ181), and by Project Program of Key Laboratory of Urban Underground Engineering of Ministry of Education (No. TUE2017-04), and by Project Program of Shandong Provincial Key Laboratory of Marine Ecology and Environment & Disaster Prevention and Mitigation (No. 201703).

References

Avramidis, I. E. and Morfidis, K. (2006). "Bending of beams on three-parameter elastic foundation." *International Journal of Solids and Structures*, Vol. 43, No. 2, pp. 357-375, DOI: 10.1016/j.ijsolstr.2005.03.033.

Basile, F. (2012). "Pile-group response under seismic loading." *Proc. 2nd International Conference on Performance-Based Design in Earthquake Geotechnical Engineering*, Taormina, Italy, pp. 28-30.

Cheng, C., Dasari, G. R., and Chow, Y. K. (2007). "Finite element analysis of tunnel-soil-pile interaction using displacement control model." *Tunnelling and Underground Space Technology*, Vol. 22, No. 4, pp. 450-466, DOI: 10.1016/j.tust.2006.08.002.

Chheng, C. and Likitlersuang, S. (2018). "Underground excavation behaviour in Bangkok using three-dimensional finite element method." *Journal Name revised as* "*Computers and Geotechnics*", Vol. 95, No. 10, pp. 68-81, DOI: 10.1016/j.compgeo.2017.09.016.

Dias, T. G. S. and Bezuijen, A. (2015). "Data analysis of pile tunnel interaction." *Journal of Geotechnical and Geoenvironmental Engineering*, Vol. 141, No. 12, pp. 04015051, DOI: 10.1061/(ASCE)GT.1943-5606.0001350.

Franza, A. and Marshall, A. M. (2018). "Centrifuge modeling study of the response of piled structures to tunneling." *Journal of Geotechnical and Geoenvironmental Engineering*, Vol. 144, No. 2, p. 04017109, DOI: 10.1061/(ASCE)GT.1943-5606.0001751.

Franza, A., Marshall, A. M., and Haji, T. (2017). "A simplified elastic analysis of tunnel-piled structure interaction." *Tunnelling and Underground Space Technology*, Vol. 61, No. 1, pp. 104-121, DOI: 10.1016/j.tust.2016.09.008.

Huang, M. and Mu, L. (2012). "Vertical response of pile-raft foundations subjected to tunnelling-induced ground movements in layered soil." *International Journal for Numerical and Analytical Methods in Geomechanics*, Vol. 36, No. 8, pp. 977-1001, DOI: 10.1002/nag.1035.

Huang, M., Zhang, C., and Li, Z. (2009). "A simplified analysis method for the influence of tunneling on grouped piles." *Tunnelling and Underground Space Technology*, Vol. 24, No. 4, pp. 410-422, DOI: 10.1016/j.tust.2008.11.005.

Jacobsz, S. W., Standing, J. R., and Mair, R. J. (2004). "Centrifuge modelling of tunnelling near driven piles." *Soils and Foundations*, Vol. 44, No. 1, pp. 49-56, DOI: 10.3208/sandf.44.49.

Kaalberg, F. J., Teunissen, E. A. H., and van Tol, A. F. (2006). "Dutch research on the impact of shield tunnelling on pile foundations." *Proc. 5th International Symposium on Geotechnical Aspects of Underground Construction in Soft Ground*, ISSMGE Amsterdam, Netherlands, pp. 123-131.

Kerr, A. D. (1965). "A study of a new foundation model." *Acta Mechanica*, Vol. 1, No. 2, pp. 135-147, DOI: 10.1007/BF01174308.

Kerr, A. D. (1985). "On the determination of foundation model parameters." *Journal of Geotechnical Engineering*, Vol. 111, No. 11, pp. 1334-1340, DOI: 10.1061/(ASCE)0733-9410(1985)111:11(1334).

Kitiyodom, P., Matsumoto, T., and Kawaguchi, K. (2005). "A simplified analysis method for piled raft foundations subjected to ground movements induced by tunnelling." *International Journal for Numerical and Analytical Methods in Geomechanics*, Vol. 29, No. 15, pp. 1485-1507, DOI: 10.1002/nag.469.

Kneifati, M. C. (1985). "Analysis of plates on a Kerr foundation model." *Journal of Engineering Mechanics*, Vol. 111, No. 11, pp. 1325-1342, DOI: 10.1061/(ASCE)0733-9399(1985)111:11(1325).

Lee, C. J. and Jacobsz, S. W. (2006). "The influence of tunneling on adjacent piled foundation." *Tunnelling and Underground Space Technology*, Vol. 21, No. 3, p. 430, DOI: 10.1016/j.tust.2005.12.072.

Lee, K. M., Rowe, R. K., and Lo, K. Y. (1992). "Subsidence owing to tunnelling. I. Estimating the gap parameter." *Canadian Geotechnical Journal*, Vol. 29, No. 6, pp. 929-940, DOI: 10.1139/t92-104.

Lee, R. G., Turner, A. J., and Whitworth, L. J. (1994). "Deformations caused by tunneling beneath a piled structure." *Proc. 13th International Conference of Soil Mechanics and Foundation Engineering*, IGC, New Delhi, India, pp.873-878.

Liang, R., Xia, T., and Lin, C. (2015). "Initial Excess pore water pressures induced by tunnelling in soft ground." *Journal of Central South University*, Vol. 22, No. 11, pp. 4300-4309, DOI: 10.1007/s11771-015-2978-8.

Liang, R., Xia, T., and Hong, Y. (2016). "Effects of above-crossing tunnelling on the existing shield tunnels." *Tunnelling and Underground Space Technology*, Vol. 58, No. 9, pp. 159-176, DOI: 10.1016/j.tust.2016.05.002.

Liang, R., Xia, T., and Huang, M. (2017). "Simplified method for evaluating the effects of adjacent excavation on shield tunnel considering the shearing effect." *Computers and Geotechnics*, Vol. 81, No. 1, pp. 167-187, DOI: 10.1016/j.compgeo.2016.08.017.

Liyanapathirana, D. S. and Nishanthan, R. (2016). "Influence of deep excavation induced ground movements on adjacent piles." *Tunnelling and Underground Space Technology*, Vol. 52, No. 2, pp. 168-181, DOI: 10.1016/j.tust.2015.11.019.

Lo, K. Y. and Rowe, R. K. (1982). *Prediction of ground subsidence due to tunneling in clays*, Research Report GEOT-10-82, University of Western Ontario, London, Ontario, Canada.

Loganathan, N. and Poulos, H. G. (1998). "Analytical prediction for tunnellinginduced ground movements in clays." *Journal of Geotechnical and Geoenvironmental Engineering*, Vol. 124, No. 9, pp. 846-856, DOI: 10.1061/(ASCE)1090-0241(1998)124:9(846).

Loganathan, N., Poulos, H. G., and Stewart, D. P. (2000). "Centrifuge model testing of tunnelling-induced ground and pile deformations." *Géotechnique*, Vol. 50, No. 3, pp. 283-294, DOI: 10.1680/geot.2000.50.3.283.

Lu, X. L., Zhou, Y. C., and Huang, M. S. (2017). "Computation of the minimum limit support pressure for the shield tunnel face stability under seepage condition." *International Journal of Civil Engineering*, Vol. 15, No. 6, pp. 849-863, DOI: 10.1007/s40999-016-0116-0.

Lu, X. L., Wang, H. R., and Huang, M. S. (2014). "Upper bound limit analysis of the face stability of shield tunnel below the water table." *Mathematical Problems in Engineering*, DOI: 10.1155/2014/727964.

Lueprasert, P., Jongpradist, P., and Jongpradist, P. (2017). "Numerical investigation of tunnel deformation due to adjacent loaded pile and pile-soil-tunnel interaction." *Tunnelling and Underground Space Technology*, Vol. 70, No. 11, pp. 166-181, DOI: 10.1016/j.tust.2017.08.006.

Mair, R. J., Taylor, R. N., and Bracegirdle, A. (1993). "Subsurface settlement profiles above tunnels in clays." *Géotechnique*, Vol. 43, No. 2, pp. 315-320, DOI: 10.1680/geot.1993.43.2.315.

Marshall, A. M., Farrell, R. P., and Klar, A. (2012). "Tunnels in sands the effect of size, depth, and volume loss on greenfield displacements." *Géotechnique*, Vol. 62, No. 5, pp. 385-399, DOI: 10.1680/geot.10.P.047.

Marshall, A. and Mair, R. (2011). "Tunneling beneath driven or jacked end-bearing piles in sand." *Canadian Geotechnical Journal*, Vol. 48, No. 12, pp. 1757-1771, DOI: 10.1139/t11-067.

Marshall, A. M. and Twana, H. (2015). "An analytical study of tunnel-pile interaction." *Tunnelling and Underground Space Technology*, Vol. 45, No. 1, pp. 43-51, DOI: 10.1016/j.tust.2014.09.001.

Miro, S., König, M., and Hartmann. (2015). "A probabilistic analysis of subsoil parameters uncertainty impacts on tunnel-induced ground movements with a back-analysis study." *Computers and Geotechnics*, Vol. 68, No. 7, pp. 38-53, DOI: 10.1016/j.compgeo.2015.03.012.

Mroueh, H. and Shahrour, I. (2002). "Three-dimensional finite element analysis of the interaction between tunnelling and pile foundations." *International Journal for Numerical and Analytical Methods in Geomechanics*, Vol. 26, No. 3, pp. 217-230, DOI: 10.1002/nag.194.

Mu, L., Huang, M., and Finno, R. J. (2012). "Tunnelling effects on lateral behavior of pile rafts in layered soil." *Tunnelling and Underground Space Technology*, Vol. 28, No. 3, pp. 192-201, DOI: 10.1016/j.tust.2011.10.010.

Ng, C. W. W., Lu, H., and Peng, S. (2012). "Three-dimensional centrifuge modelling of the effects of twin tunnelling on an existing pile." *Tunnelling and Underground Space Technology*, Vol. 35, No. 4, pp. 189-199, DOI: 10.1016/j.tust.2012.07.008.

Pasternak, P. L. (1954). *On a new method of analysis of an elastic foundation by means of two-constants,* State Architecture & Construction Press, Moscow, Russia.

Peck, R. B. (1969). "Deep excavations and tunneling in soft ground." *Proc., 7th International Conference on Soil Mechanics and Foundation Engineering*, Mexico City, Mexico, pp. 225-290.

Rowe, R. K. and Kack, G. J. (1983). "A theoretical examination of the settlements induced by tunnelling: Four case histories." *Canadian Geotechnical Journal*, Vol. 20, No. 2, pp. 299-314, DOI: 10.1139/t83-033.

Sagaseta, C. (1987). "Analysis of undrained soil deformation due to ground loss." *Géotechnique*, Vol. 37, No. 3, pp. 301-320, DOI: 10.1680/geot.1987.37.3.301.

Selemetas, D. (2005). *The response of full-scale piles and piled structures to tunnelling*, PhD Thesis, University of Cambridge, Cambridge, England.

Shakeel, M. and Ng, C. W. W. (2018). "Settlement and load transfer mechanism of a pile group adjacent to a deep excavation in soft clay." *Journal Name revised as* "*Computers and Geotechnics*", Vol. 96, No. 4, pp. 55-72, DOI: 10.1016/j.compgeo.2017.10.010.

Soomro, M. A., Hong, Y., and Ng, C. W. W. (2015). "Load transfer mechanism in pile group due to single tunnel advancement in stiff clay." *Tunnelling and Underground Space Technology*, Vol. 45, No. 1, pp. 63-72, DOI: 10.1016/j.tust.2014.08.001.

Soomro, M. A., Ng, C. W. W., and Liu, K. (2017). "Pile responses to side-by-side twin tunnelling in stiff clay: Effects of different tunnel depths relative to pile." *Computers and Geotechnics*, Vol. 84, No. 4, pp. 101-116, DOI: 10.1016/j.compgeo.2016.11.011.

Verruijt, A. and Booker, J. R. (1996). "Surface settlement due to deformation of a tunnel in an elastic half plane." *Géotechnique*, Vol. 46, No. 4, pp. 753-756, DOI: 10.1680/geot.1996.46.4.753.

Vesic, A. B. (1961). "Beam on elastic subgrade and the Winkler's hypothesis." *Proc. Fifth International Conference of Soil Mechanics and Foundation Engineering,* ISSMGE, Paris, France, pp. 845-851.

Wang, S. Y., Yang, J. S., and Yang, Y. H. (2014). "Construction of large-span twin tunnels below a high-rise transmission tower: A case study." *Geotechnical and Geological Engineering*, Vol. 32, No. 2, pp. 453-467, DOI: 10.1007/s10706-013-9726-3.

Xu, K. J. and Poulos, H. G. (2001). "3-D elastic analysis of vertical piles subjected to 'passive' loadings." *Computers and Geotechnics*, Vol. 28, No. 5, pp. 349-375, DOI: 10.1016/S0266-352X(00)00024-0.

Yu, H. and Rowe, R. K. (1999). "Plasticity solutions for soil behaviour around contracting cavities and tunnels." *International Journal for Numerical and Analytical Methods in Geomechanics*, Vol. 23, No. 12, pp. 1245-1279, DOI: 10.1002/(SICI)1096-9853(199910)23:12 <1245::AID-NAG30>3.3.CO;2-N.

Zhang, Z. G., Huang, M. S., Xu, C., Jiang, Y. J., and Wang, W. D. (2018). "Simplified solution for tunnel-soil-pile interaction in Pasternak's foundation model." *Tunnelling and Underground Space Technology*, Vol. 78, No. 8, pp. 146-158, DOI: 10.1016/j.tust.2018.04.025.

Zhang, Z. G. and Zhang, M. X. (2013). "Mechanical effects of tunneling on adjacent pipelines based on Galerkin solution and layered transfer matrix solution." *Soils and Foundations*, Vol. 53, No. 4, pp. 557-568, DOI: 10.1016/j.sandf.2013.06.007.

Zhang, Z. G., Zhang, M. X., and Jiang, Y. J. (2017). "Analytical prediction for ground movements and liner internal forces induced by shallow tunnels considering non-uniform convergence pattern and ground-liner interaction mechanism." *Soils and Foundations*, Vol. 57, No. 2, pp. 211-226, DOI: 10.1016/j.sandf.2017.03.004.